JACS
JOURNAL OF THE AMERICAN CHEMICAL SOCIETY
Article
pubs.acs.org/JACS

A Supramolecular Janus Hyperbranched Polymer and Its Photoresponsive Self-Assembly of Vesicles with Narrow Size Distribution

Yong Liu,[†,‡] Chunyang Yu,[†,‡] Haibao Jin,[†] Binbin Jiang,[†] Xinyuan Zhu,[†] Yongfeng Zhou,*[,†] Zhongyuan Lu,*[,§] and Deyue Yan[†]

[†]School of Chemistry and Chemical Engineering, State Key Laboratory of Metal Matrix Composites, Shanghai Jiao Tong University, 800 Dongchuan Road, Shanghai 200240, P. R. China

[§]Institute of Theoretical Chemistry, State Key Laboratory of Theoretical and Computational Chemistry, Jilin University, Changchun 130023, P. R. China

Supporting Information

ABSTRACT: Herein, we report a novel Janus particle and supramolecular block copolymer consisting of two chemically distinct hyperbranched polymers, which is coined as Janus hyperbranched polymer. It is constructed by the noncovalent coupling between a hydrophobic hyperbranched poly(3-ethyl-3-oxetanemethanol) with an apex of an azobenzene (AZO) group and a hydrophilic hyperbranched polyglycerol with an apex of a β-cyclodextrin (CD) group through the specific AZO/CD host–guest interactions. Such an amphiphilic supramolecular polymer resembles a tree together with its root very well in the architecture and can further self-assemble into unilamellar bilayer vesicles with narrow size distribution, which disassembles reversibly under the irradiation of UV light due to the *trans*-to-*cis* isomerization of the AZO groups. In addition, the obtained vesicles could further aggregate into colloidal crystal-like close-packed arrays under freeze-drying conditions. The dynamics and mechanism for the self-assembly of vesicles as well as the bilayer structure have been disclosed by a dissipative particle dynamics simulation.

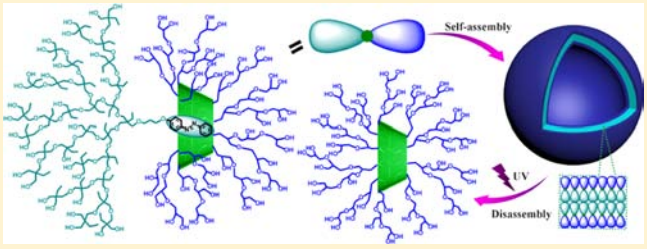

1. INTRODUCTION

Since the term of "Janus grains" was coined by de Gennes in his Nobel lecture two decades ago,[1] Janus particles have attracted extensive attention owing to their unique and fascinating properties correlated to their asymmetric structure and functionalization as well as their great potentials to be used as new building blocks in self-assembly.[2−8] And thus, it has recently become a very challenging and attractive research field to seek for new Janus particles. Janus dendrimers are a kind of special Janus particles consisting of two chemically distinct dendrons in a single molecule.[9−12] Goodby and Percec et al. have greatly pushed forward the bulk or solution self-assembly of Janus dendrimers by endowing them with amphiphilic characters.[13−18] For the bulk self-assembly, Goodby found the Janus liquid crystalline dendrimers could exhibit chiral nematic and chiral smectic C phases in bulk.[13,14] Percec and co-workers obtained more complex bilayered pyramidal or vesicular columns from the self-assembly of semifluorinated Janus dendrimers.[15,16] For the solution self-assembly, Percec and co-workers synthesized libraries of amphiphilic Janus dendrimers and found these compounds spontaneously self-assembled into a rich palette of morphologies in water, including vesicles (denoted as dendrimersomes), cubosomes, disks, tubular vesicles, and helical ribbons.[19,20] These unique self-assembly behaviors make Janus dendrimers very promising in biomedical applications including mimicking primitive biological membranes, configuring into biomimetic nanocapsules, fabricating functional nanomedicines, and so on.[19−23] However, the usually time-consuming synthesis process of monodendrons is an undeniable and unavoidable barrier to progress. As we know, besides dendrimers, there is still another big category of dendritic polymers, namely hyperbranched polymers (HBPs). HBP is rather irregular when compared with its dendrimer analogue; however, it has some advantages of facile one-pot synthesis, low cost, and many varieties. Thus, it seems meaningful and possible to prepare Janus HBPs (JHBPs), which can be considered as a cousin of Janus dendrimers. To our great surprise, although a large population of HBPs with different architectures and topologies has been synthesized,[24−26] no JHBP has been reported up to now.

The difficulty in synthesizing JHBPs is understandable. Janus dendrimers can be obtained by covalent coupling of two dendrons through the reactions between the focal point functionalities or apexes. However, different to dendrons, it is not easy to get monoreactive HBP since the apex in HBP will be destroyed by the intramolecular cyclization during the "one-

Received: December 16, 2012
Published: March 6, 2013

   dx.doi.org/10.1021/ja3122608 | J. Am. Chem. Soc. 2013, 135, 4765−4770

Scheme 1. Preparation, Self-Assembly and Disassembly Processes of the Supramolecular JHBP of HBPO-*b*-HPG

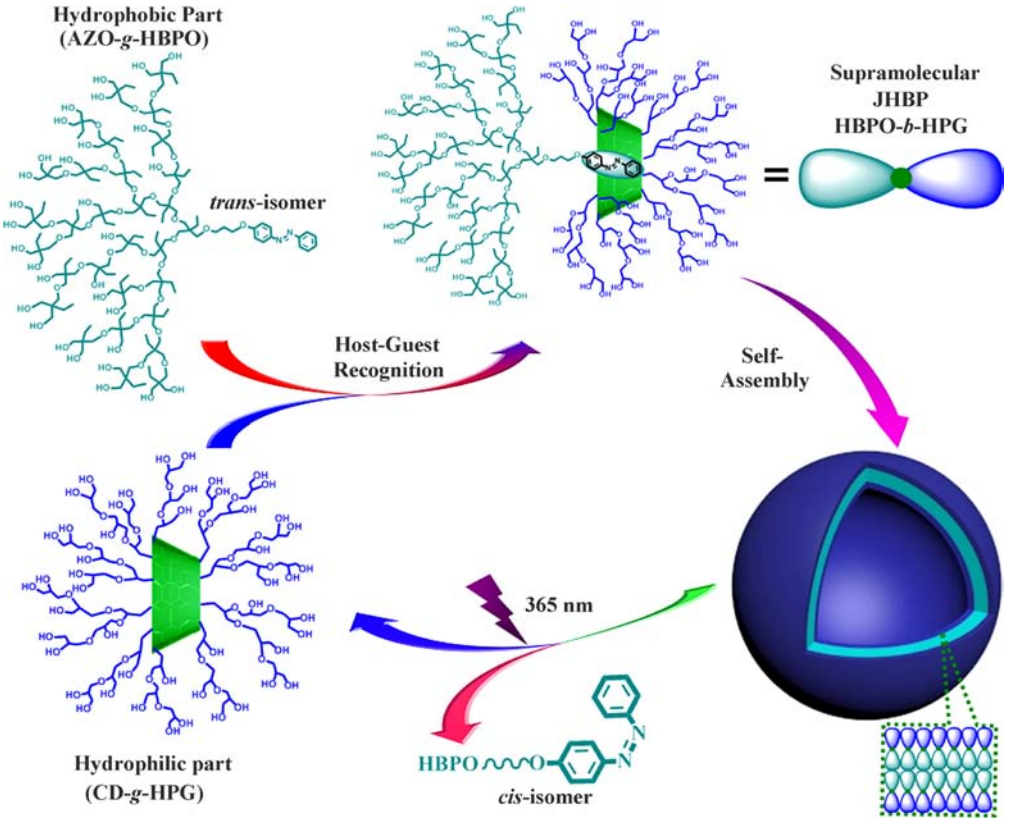

pot" synthesis process,[27,28] which has become the biggest obstacle to synthesize JHBPs through covalent bonding. Recently, supramolecular polymers formed by connecting micromolecular or polymeric segments through noncovalent bonds have received much attention, which have proved to be a new and powerful way to get polymers with various architectures and functions.[29−41] As a unique example, Fréchet et al. reported a supramolecular Janus dendrimer by multiple hydrogen bonds and electrostatic interactions between a polyester dendron having a carboxylic acid apex and a polyester dendron having a bis-adamanthyl urea apex.[42] As inspired by them, it is greatly expected that the specific noncovalent binding may be an alternative and even more practical way to prepare JHBP.

Very recently, our group reported a hydrophilic hyperbranched polyglycerol with a β-cyclodextrin apex (CD-*g*-HPG) by using β-CD as a multihydroxyl initiator to initiate the anionic ring-opening multibranching polymerization of glycerol.[36] On the basis of it, this paper reports the first example of supramolecular JHBP by the complexation between CD-*g*-HPG and hyperbranched poly(3-ethyl-3-oxetanemethanol) (HBPO) with an apex of an azobenzene group (AZO-*g*-HBPO) through specific AZO/CD host−guest interactions (Scheme 1). The obtained supramolecular JHBP of HBPO-*b*-HPG further self-assembled into narrowly distributed vesicles in water under visible light, and alternatively, the vesicles could disassemble into unimers under the irradiation of UV light. In addition, a dissipative particle dynamics (DPD) simulation study on the self-assembly of HBPO-*b*-HPG was preformed, which disclosed the dynamics of the self-assembly and the detailed structure of the vesicles.

2. RESULTS AND DISCUSSION

CD-*g*-HPG ($M_{n,GPC}$ = 3000 Da, $M_{n,NMR}$ = 5700 Da, DP_n = 62, PDI = 1.31, DB = 0.65) was synthesized according to our previously work (Figures S1−S4).[36] AZO-*g*-HBPO ($M_{n,GPC\text{-}MALLS}$ = 9400 Da, $M_{n,NMR}$ = 14 000 Da, DP_n = 120, PDI = 1.40, DB = 0.46) was synthesized by the cationic ring-opening multibranching polymerization of 3-ethyl-3-oxetanemethanol monomers, by using 4-(3-hydroxypropyloxy)-azobenzene (AZO−OH) as a monohydroxyl initiator and a slow monomer addition technique (Figures S5−S9). The slow addition of monomers ensured that a high instantaneous conversion and low monomer concentration were kept at all reaction times, which favored the activated monomer (AM) mechanism and more dendritic segments.[28] Meanwhile, it also increased the probability of the monomers to react with the end hydroxyl groups of the AZO−OH, preventing the formation of HBPO homopolymers. The CD groups of CD-*g*-HPGs were found capable to host the guest molecules in spite of the steric hindrance of the grafted HPG chains (Figure S10), so the complexation between CD-*g*-HPGs and AZO-*g*-HBPOs into supramolecular JHBPs of HBPO-*b*-HPGs through the specific CD/AZO molecular recognition interactions is well expected.

The complexation and self-assembly of CD-*g*-HPG and AZO-*g*-HBPO (molar ratio of CD: AZO = 1:1) were performed by adding water dropwise into a DMF solution of them and were monitored by dynamic light scattering (DLS) measurements (Figure 1a,b). A unimodal distribution with increasing the average hydrodynamic diameter (D_h) was observed when the volume percentage ratio of water/DMF was increased from 0% to 26% (Figure 1a), followed with the increase of solution opacity as well as Tyndall scattering (Figure 1b). The change of D_h of the aggregates (Figure 1b) could be

dx.doi.org/10.1021/ja3122608 | J. Am. Chem. Soc. 2013, 135, 4765−4770

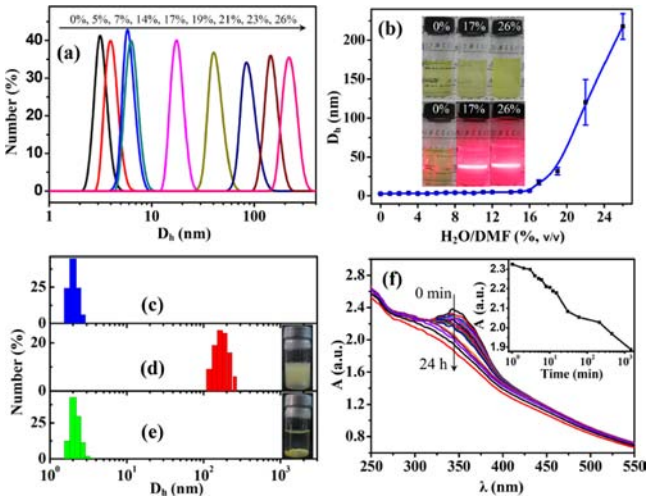

Figure 1. Complexation, self-assembly, and disassembly of the polymers. (a) DLS results of the mixed solution with different water/DMF volume percentage ratios (v/v). (b) Dependence of D_h on the water/DMF ratios. Insets show the photos of the mixed solution with three water contents. (c) Number-averaged size distribution of the aqueous solution of CD-*g*-HPG. (d) The solution of HBPO-*b*-HPG self-assemblies (inset) and the number-averaged size distribution. (e) The residual transparent solution after UV irradiation (inset) and the number-averaged size distribution. (f) UV−vis spectra of HBPO-*b*-HPG aqueous solution with different UV irradiation time (λ = 365 nm). Inset shows the absorbance at λ = 349 nm (*trans*-AZO) versus UV irradiation time.

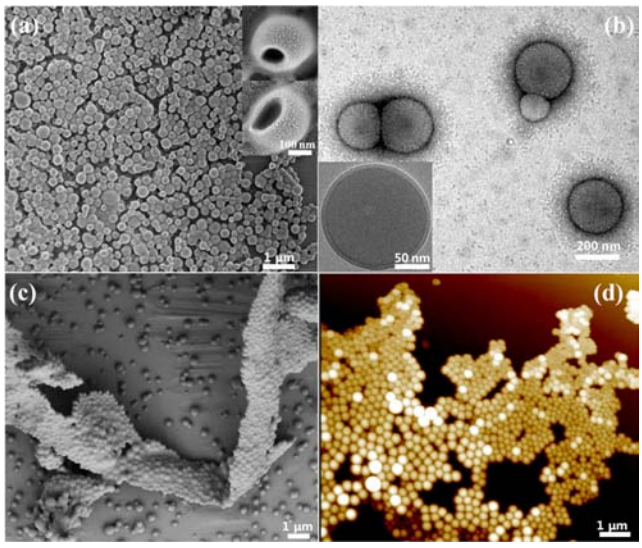

Figure 2. Self-assemblies captured by (a,c) SEM, (b) TEM, and (d) AFM. The inset in (a) shows the SEM images of the particles with holes, and the inset in (b) shows the TEM image of the freeze-dried particles.

divided into two stages. In the first stage (water/DMF: 0−15%), a small increase of the D_h from 2.7 to 5.1 nm was observed. CD-*g*-HPGs and AZO-*g*-HBPOs existed as the unimers around 2.7 nm in the cosolvent of DMF. The D_h of 5.1 nm is close to the size of the 1:1 complex of CD-*g*-HPG and AZO-*g*-HBPO. Thus, this stage is attributed to the 1:1 complexation between CD-*g*-HPGs and AZO-*g*-HBPO through AZO/CD interactions to form the supramolecular HBPO-*b*-HPG. Such a complexation process is also proved by 2D NOESY spectrum (Figure S11), which indicates the intermolecular correlations between the internal H3, H5 protons in the inner caves of CDs and the protons of AZO groups. In the second stage (water/DMF: 16−26%), a rapid increase of the D_h into 220 nm and solution opacity was observed, which strongly supported that the obtained HBPO-*b*-HPGs further self-assembled into supramolecular aggregates in this stage.

To obtain the stable supramolecular aggregates, the polymer solution with a water/DMF ratio of 25% (v/v) was dialyzed against water to remove DMF, and a final bluish yellow solution with a polymer concentration of 1 mg/mL was obtained. The obtained aggregates have a nearly monodisperse size distribution with the PDI around 0.004 through the DLS measurement (Figure 1d), and the D_h is kept at 220 nm. ^{1}H NMR measurement of the freezing dried aggregates indicates they are composed of AZO-*g*-HBPO and CD-*g*-HPG with a molar ratio of 1:1 (Figure S12). The morphology of the aggregates was observed by SEM, TEM, and AFM (Figure 2). The SEM image in Figure 2a indicates the aggregates are spherical particles with a narrow size distribution, and the inner hollow structure can be directly seen according to the holes of the destroyed particles (insets of Figure 2a), which indicates the particles are vesicles or hollow spheres. The TEM images (Figure 2b and Figure S13) of the air-dried aggregates stained by phosphotungstic acid prove they are unilamellar vesicles in nature according to a clear contrast difference between the inner pool and the outer black thin wall.[43,44] Alternatively, more regular spherical vesicles with a lower contrast difference were observed (inset of Figure 2b) when the sample was only freeze-dried without staining. The cryo-TEM images (Figure S14) further demonstrate the particles are vesicular structure according to the clear skin/pool structure. The vesicle wall thickness is almost uniform and around 9.8 ± 0.8 nm through the statistical analysis of 30 vesicles from the TEM images, which agrees well with that measured by AFM (9.5 nm, Figure S15). Considering that the extended length of HBPO-*b*-HPG is around 4.8 nm based on the calculation (Figure S16) and 5.1 nm according to the DLS measurement (Figure 1b), the vesicles may possess a bilayer structure as shown in Scheme 1. The obtained vesicles have a narrowly distributed size and could further aggregate into 2D or 3D close-packed arrays under freeze-drying conditions according to the SEM (Figure 2c), TEM (Figure S17), and AFM (Figure 2d) images, which are reminiscent of the formation of the colloidal crystal from monodisperse particles. In fact, to our knowledge, both synthetic and natural vesicles are typically polydisperse, and the narrowly distributed vesicles have seldom been reported,[19,45] while neither have the vesicle colloidal crystals.

As we know, AZO groups can undergo light-triggered reversible isomerization between *trans*- and *cis*-forms under alternating visible and UV light irradiation. Only *trans*-AZO can form host−guest inclusion with *β*-CD, whereas *cis*-AZO cannot.[46,47] Thus, the UV irradiation will induce the scission of the supramolecular HBPO-*b*-HPGs, leading to the disassembly of the vesicles. As proof-of-principle experiments, under the irradiation of UV light (λ = 365 nm, 250 W) for 15 min, the HBPO-*b*-HPG polymer solution was transformed from turbid (Figure 1d) with a D_h = 220 nm to transparent with a D_h = 2 nm (Figure 1e). Meanwhile, some yellow precipitates were observed (inset of Figure 1e), which are attributed to the insoluble and pure AZO-*g*-HBPOs based on the ^{1}H NMR results (Figure S18). The residuals inside the

dx.doi.org/10.1021/ja3122608 | J. Am. Chem. Soc. 2013, 135, 4765−4770

transparent solution after irradiation are believed to be the unimers of CD-*g*-HPGs according to the UV−vis spectrum (Figure S19) and ^{1}H NMR result (Figure S20) as well as the fact of the same D_h with that of pure CD-*g*-HPG aqueous solution (Figure 1c). In addition, the UV−vis spectra of the self-assembly system (Figure 1f) show that there is a clear decrease in the absorbance of the peak at λ = 349 nm attributed to *trans*-AZO groups with the increase of UV irradiation time (λ = 365 nm, 8 W). Thus, it can be concluded that the HBPO-*b*-HPG vesicles disassemble into CD-*g*-HPG unimers and AZO-*g*-HBPO precipitates in water under the UV irradiation due to the *trans*-to-*cis* transition of the AZO groups (Scheme 1). It should be noted that there is no significant increase of the peaks at λ = 450 nm attributed to *cis*-AZO groups probably because the disassociated AZO-*g*-HBPOs after *trans*-to-*cis* transformation were directly precipitated from the solution.

The colloidal stability of the obtained vesicles is excellent, even under the competitive molecules and heating process. No evident changes in both size and morphology were observed when the vesicle solution was kept at the room temperature for half a year according to the DLS and SEM measurements (Figures S21 and S22). In addition, if competitive guest molecules of AD-COONa and AZO-Na or the competitive host molecules of α-CD and β-CD, which have a stronger complexation capacity to the CD or AZO groups in the so-prepared supramolecular HBPO-*b*-HPGs, were added to the self-assembly system, no significant difference in the DLS results was observed when compared with that of the initial HBPO-*b*-HPG vesicle solution (Figure S23). Besides, no significant difference was observed when the solution was heated from 20 to 70 °C according to temperature-variable DLS measurements (Figure S24).

The above experiments reveal an interesting phenomenon that the supramolecular HBPO-*b*-HPGs could self-assemble into vesicles by adding water dropwise into the polymer DMF solution. To verify the experimental results and to understand the mechanism of spontaneous vesicle formation, a DPD simulation was performed to explore the self-assembly process of HBPO-*b*-HPGs. In order to capture the essential feature of HBPO-*b*-HPG, a model molecule $A_{57}CB_{14}$, as shown in Figure 3a, is constructed in the DPD simulations. Three "A" beads represent two repeating units in the hydrophobic HBPO segments, while one "B" bead refers to one repeating unit in the hydrophilic HPG segment. The "C" bead refers to the connector consisting of the CD/AZO group, and the subscript numbers of 57 and 14 refer to the number of the DPD beads. The details of the simulation model and method are described in the Supporting Information.

Figure 3 displays the snapshots in the self-assembly process through the DPD simulation. After the initially homogeneous state (Figure 3b), the amphiphilic JHBPs aggregate into a large irregular aggregate with lamella structure at 0.780 μs (Figure 3c). Then, the large irregular aggregate gradually changes to a hollow vesicular shape with holes penetrating through the vesicle membrane at 1.040 μs (Figure 3d). The vesicle turns more regular with the holes closing from 1.456, 1.768, to 2.028 μs (Figure 3e−g, respectively). At t = 4.160 μs, the vesicle is completely sealed with a spherical shape (Figure 3h). These simulation results reflect the vesicle formation pathway of JHBPs is similar to that of Janus dendrimers.[19]

The simulation results can provide more details of the vesicle structure. Figure 4a,b clearly shows the bilayer membrane structure of the vesicle, in which the hydrophilic HPG blocks

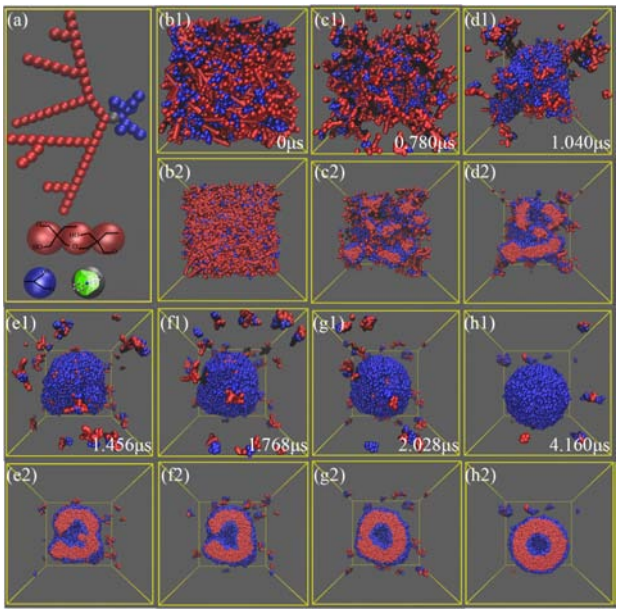

Figure 3. DPD simulations on the self-assembly of the supramolecular HBPO-*b*-HPG. (a) The schematic model $A_{57}CB_{14}$ for one HBPO-*b*-HPG molecule. (b) The initial snapshot showing randomly distributed HBPO-*b*-HPG molecules in solution. (c and d) Snapshots showing the formation of a large irregular aggregate with lamellar structure and a bilayer structure. (e) The snapshot showing the formation of a hollow vesicular aggregate with holes penetrating through the vesicle membrane. (f and g) Snapshots showing the molecule rearrangement and the vesicle closing. (h) The snapshot showing the final vesicle structure. For each image from (b−h), the upper one is the 3D view, while the lower one is the cross-section view. The solvent beads are removed for clarity. Red, HBPO; blue, HPG; gray, CD/AZO group.

distribute in the internal and the external surfaces of the vesicle, while the hydrophobic HBPO blocks form the inner "wall" of the vesicle. Furthermore, the density distribution from the center of mass to the outside of the vesicle was calculated to characterize the vesicle microstructure. As can be seen in Figure 4c, the density distribution profile of HPG segments has two peaks, while the density distribution profile of HBPO has only one smooth peak. Moreover, the first peak of HPG is slightly higher than the second peak, which means that the density of internal vesicle surface is slightly larger than that of the external vesicle surface. We can also calculate the membrane thickness of the vesicle from the density distribution profile. The calculated membrane thickness of the vesicle is 9.23 nm, which is well consistent with the experimental result.

3. CONCLUSIONS

In summary, we have reported supramolecular Janus hyperbranched polymers through noncovalent host−guest coupling between the AZO-functionalized HBPOs and CD-functionalized HPGs. The obtained supramolecular amphiphiles further self-assemble into vesicles in water, which can be disassembled under irradiation of UV light (365 nm). In addition, the computer simulation results deepen our understandings of the self-assembly process and the vesicular structure and are consistent with the experimental results. We believe the present work will cast a new light on the design, synthesis, and self-assembly of hyperbranched-based supramolecular polymers with more complex topologies or architectures.

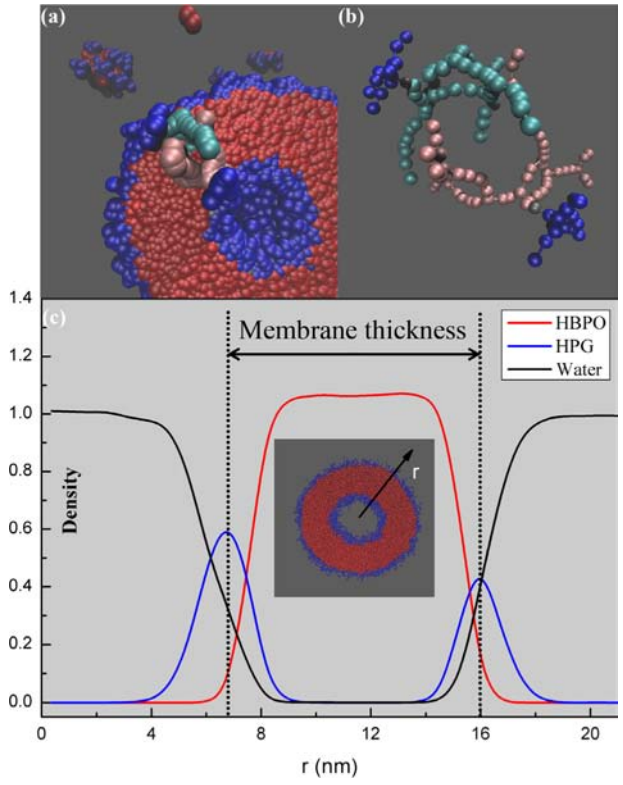

Figure 4. The vesicular structure by the DPD simulation. (a) A cross-section view of one vesicle showing the bilayer structure. (b) Two labeled molecules extracted from the bilayer to show the molecular packing model. (c) Radial density distributions of the HBPO (red) and HPG (blue) components in the vesicle. The distance from the center of mass of the vesicle to the outside of the vesicle is *r*. Membrane thickness is defined as the distance between the peaks of density distribution of the HPG segments located at the internal leaflet and at the external leaflet.

■ ASSOCIATED CONTENT

Ⓢ Supporting Information

Experimental materials and instruments; synthesis and characterizations of CD-*g*-HPG, AZO-*g*-HBPO, and supramolecular HBPO-*b*-HPG; TEM, cryo-TEM and AFM images of the vesicles. This material is available free of charge via the Internet at http://pubs.acs.org.

■ AUTHOR INFORMATION

Corresponding Author

yfzhou@sjtu.edu.cn; luzhy@jlu.edu.cn

Author Contributions

‡These authors contributed equally.

Notes

The authors declare no competing financial interest.

■ ACKNOWLEDGMENTS

We thank the China National Funds for Distinguished Young Scientists (21225420), National Basic Research Program (2009CB930400, 2012CB821500, 2013CB834506), National Natural Science Foundation of China (21074069, 91127047), and Shanghai Rising-Star Program (11QH1401500).

■ REFERENCES

(1) de Gennes, P.-G. *Angew. Chem., Int. Ed.* **1992**, *31*, 842−845.
(2) Walther, A.; Müller, A. H. E. *Soft Matter* **2008**, *4*, 663−668.
(3) Gröschel, A. H.; Schacher, F. H.; Schmalz, H.; Borisov, O. V.; Zhulina, E. B.; Walther, A.; Müller, A. H. *Nat. Commun.* **2012**, *3*, 710−710.
(4) Chen, Q.; Whitmer, J. K.; Jiang, S.; Bae, S. C.; Luijten, E.; Granick, S. *Science* **2011**, *331*, 199−202.
(5) Yan, J.; Bloom, M.; Bae, S. C.; Luijten, E.; Granick, S. *Nature* **2012**, *491*, 578−581.
(6) Du, J.; O'Reilly, R. K. *Chem. Soc. Rev.* **2011**, *40*, 2402−2416.
(7) Li, Y.; Zhang, W.-B.; Hsieh, I. F.; Zhang, G.; Cao, Y.; Li, X.; Wesdemiotis, C.; Lotz, B.; Xiong, H.; Cheng, S. Z. D. *J. Am. Chem. Soc.* **2011**, *133*, 10712−10715.
(8) Jiang, S.; Chen, Q.; Tripathy, M.; Luijten, E.; Schweizer, K. S.; Granick, S. *Adv. Mater.* **2010**, *22*, 1060−1071.
(9) Hawker, C. J.; Fréchet, J. M. J. *J. Am. Chem. Soc.* **1992**, *114*, 8405−8413.
(10) Wooley, K. L.; Hawker, C. J.; Fréchet, J. M. J. *J. Chem. Soc., Perkin Trans. 1* **1991**, 1059−1076.
(11) Rosen, B. M.; Wilson, C. J.; Wilson, D. A.; Peterca, M.; Imam, M. R.; Percec, V. *Chem. Rev.* **2009**, *109*, 6275−6540.
(12) Caminade, A.-M.; Laurent, R.; Delavaux-Nicot, B.; Majoral, J.-P. *New J. Chem.* **2012**, *36*, 217−226.
(13) Saez, I. M.; Goodby, J. W. *Chem. Commun.* **2003**, 1726−1727.
(14) Saez, I. M.; Goodby, J. W. *Chem.—Eur. J.* **2003**, *9*, 4869−4877.
(15) Percec, V.; Imam, M. R.; Bera, T. K.; Balagurusamy, V. S. K.; Peterca, M.; Heiney, P. A. *Angew. Chem., Int. Ed.* **2005**, *44*, 4739−4745.
(16) Percec, V.; Imam, M. R.; Peterca, M.; Leowanawat, P. *J. Am. Chem. Soc.* **2012**, *134*, 4408−4420.
(17) Bury, I.; Heinrich, B.; Bourgogne, C.; Guillon, D.; Donnio, B. *Chem.—Eur. J.* **2006**, *12*, 8396−8413.
(18) Lenoble, J.; Campidelli, S.; Maringa, N.; Donnio, B.; Guillon, D.; Yevlampieva, N.; Deschenaux, R. *J. Am. Chem. Soc.* **2007**, *129*, 9941−9952.
(19) Percec, V.; Wilson, D. A.; Leowanawat, P.; Wilson, C. J.; Hughes, A. D.; Kaucher, M. S.; Hammer, D. A.; Levine, D. H.; Kim, A. J.; Bates, F. S.; Davis, K. P.; Lodge, T. P.; Klein, M. L.; DeVane, R. H.; Aqad, E.; Rosen, B. M.; Argintaru, A. O.; Sienkowska, M. J.; Rissanen, K.; Nummelin, S.; Ropponen, J. *Science* **2010**, *328*, 1009−1014.
(20) Peterca, M.; Percec, V.; Leowanawat, P.; Bertin, A. *J. Am. Chem. Soc.* **2011**, *133*, 20507−20520.
(21) Sun, L.; Ma, X.; Dong, C. M.; Zhu, B.; Zhu, X. *Biomacromolecules* **2012**, *13*, 3581−3591.
(22) Nierengarten, J.-F.; Eckert, J.-F.; Rio, Y.; del Pilar Carreon, M.; Gallani, J.-L.; Guillon, D. *J. Am. Chem. Soc.* **2001**, *123*, 9743−9748.
(23) Khandare, J.; Calderon, M.; Dagia, N. M.; Haag, R. *Chem. Soc. Rev.* **2012**, *41*, 2824−2848.
(24) Gao, C.; Yan, D. *Prog. Polym. Sci.* **2004**, *29*, 183−275.
(25) Carlmark, A.; Hawker, C.; Hult, A.; Malkoch, M. *Chem. Soc. Rev.* **2009**, *38*, 352−362.
(26) Voit, B. I.; Lederer, A. *Chem. Rev.* **2009**, *109*, 5924−5973.
(27) Bednarek, M.; Kubisa, P.; Penczek, S. *Macromolecules* **2001**, *34*, 5112−5119.
(28) Rahm, M.; Westlund, R.; Eldsäter, C.; Malmström, E. *J. Polym. Sci., Part A: Polym. Sci.* **2009**, *47*, 6191−6200.
(29) Hofmeier, H.; Schubert, U. S. *Chem. Soc. Rev.* **2004**, *33*, 373−399.
(30) Chen, D.; Jiang, M. *Acc. Chem. Res.* **2005**, *38*, 494−502.
(31) Huang, F.; Scherman, O. A. *Chem. Soc. Rev.* **2012**, *41*, 5879−5880.
(32) Yang, S. K.; Ambade, A. V.; Weck, M. *Chem. Soc. Rev.* **2011**, *40*, 129−137.
(33) Zhang, X.; Wang, C. *Chem. Soc. Rev.* **2011**, *40*, 94−101.
(34) Aida, T.; Meijer, E. W.; Stupp, S. I. *Science* **2012**, *335*, 813−817.
(35) Rauwald, U.; Scherman, O. A. *Angew. Chem., Int. Ed.* **2008**, *47*, 3950−3953.
(36) Tao, W.; Liu, Y.; Jiang, B.; Yu, S.; Huang, W.; Zhou, Y.; Yan, D. *J. Am. Chem. Soc.* **2012**, *134*, 762−764.
(37) Yan, Q.; Yuan, J.; Cai, Z.; Xin, Y.; Kang, Y.; Yin, Y. *J. Am. Chem. Soc.* **2010**, *132*, 9268−9270.

(38) Yang, S. K.; Ambade, A. V.; Weck, M. *J. Am. Chem. Soc.* **2010**, *132*, 1637−1645.
(39) Moughton, A. O.; O'Reilly, R. K. *Macromol. Rapid Commun.* **2010**, *31*, 37−52.
(40) de Greef, T. F. A.; Meijer, E. W. *Nature* **2008**, *453*, 171−173.
(41) Wang, C.; Wang, Z.; Zhang, X. *Acc. Chem. Res.* **2012**, *45*, 608−618.
(42) Gillies, E. R.; Fréchet, J. M. J. *J. Org. Chem.* **2003**, *69*, 46−53.
(43) Wilson, D. A.; Nolte, R. J. M.; van Hest, J. C. M. *J. Am. Chem. Soc.* **2012**, *134*, 9894−9897.
(44) Wilson, D. A.; Nolte, R. J. M.; van Hest, J. C. M. *Nature Chem.* **2012**, *4*, 268−274.
(45) Jin, H.; Huang, W.; Zhu, X.; Zhou, Y.; Yan, D. *Chem. Soc. Rev.* **2012**, *41*, 5986−5997.
(46) Jin, H.; Zheng, Y.; Liu, Y.; Cheng, H.; Zhou, Y.; Yan, D. *Angew. Chem., Int. Ed.* **2011**, *50*, 10352−10356.
(47) Nalluri, S. K. M.; Voskuhl, J.; Bultema, J. B.; Boekema, E. J.; Ravoo, B. J. *Angew. Chem., Int. Ed.* **2011**, *50*, 9747−9751.